correct metal state splitting.

Full DCCI calculations for $RuH^+$ were excessively large and were not performed. The bond energy for $RuH^+$ was obtained as follows. The difference between the DCCI-GEOM and DCCI bond energies for other largely "d-bonded" species is 1.6 kcal/mol for $PdH^+$, 1.0 kcal/mol for $RhH^+$, and 0.0 kcal/mol for $MoH^+$ (with the DCCI-GEOM energies larger than the DCCI results). Thus, $RuH^+$ was assigned a difference of 0.5 kcal/mol which was subtracted from the DCCI-GEOM result.

**Intrinsic Bond Dissociation Energies.** To obtain intrinsic s-like or d-like bond dissociation energies, the mixing of s and d character must be restricted while allowing other orbital readjustments to occur. The calculation method thus depends on the particular system. For $SrH^+$–$MoH^+$, formation of an s bond leads to an empty $d_{z^2}$ orbital while formation of a d bond leads to an empty s orbital. The calculations were thus carried out by eliminating the 5s or $4d_{z^2}$ basis functions. The bond length was then optimized under these conditions and the bond dissociation energy determined by dissociating the molecule to fragments where the same basis functions were removed from the metal ion calculation.

For $TcH^+$–$CdH^+$ the state involving an s bond is complicated by the presence of nonbonding $\sigma$ electrons. The $d_{z^2}$ basis functions could thus not be removed. For $TcH^+$–$AgH^+$ the rehybridization process was effectively removed by placing one electron in a $d_{z^2}$ orbital optimized for the corresponding state of the metal ion and freezing this orbital in the predetermined shape while allowing the other orbitals on the molecule to vary. The bonding orbital is thus forced to become orthogonal to the $d_{z^2}$ orbital. For $CdH^+$ the GVB-PP(1/2) results are used since very little d character is present. The d bonding for $TcH^+$–$PdH^+$ is determined by bonding hydrogen to the $d^n$ configuration of the metal, while for $AgH^+$ and $CdH^+$ there is effectively no d bonding due to the full $d^{10}$ shell.

These restricted calculations are at the GVB perfect pairing level and *not* the DCCI level used for reliable bond dissociation energies. Only the trends involved should be considered. The actual intrinsic bond energies presented in Table V are obtained from the GVB-PP calculations plus adding in the total amount of s–d or d–d exchange energy lost on bonding (determined from the metal ion exchange energies and the metal electronic configuration) and any electronic promotion energy.

**$MH^+$ Electronic State Splitting Calculations.** The relative energies of the low-lying electronic states of the metal hydride ions are determined by the difference in bond dissociation energies calculated for the various states at the DCCI-GEOM level of calculation. The relative bond dissociation energies were used as a measure of energy differences for the electronic states since the dissociation consistent nature of these calculations helps to remove errors inherent in the basis set representations of the metal ion states.

## IV. Conclusion

The results presented here for the second-row transition-metal hydrides form a consistent and systematic set of data which should be helpful both for understanding the complex factors involved in metal bonding and as a contribution to the increasing data base of thermodynamic and spectroscopic values for metal compounds. The ideas used to discuss the bonding in the metal hydride diatomics are also applicable for other more complicated metal-containing species. The consistent nature of the data for the entire row should be useful in helping to extract further reliable thermodynamic information from ion beam studies, increase understanding of the differences in reactivity of ground and excited states, and shed light on the reactivity differences of the different transition metals.

**Acknowledgment.** We thank the National Science Foundation (Grants CHE83-18041 and CHE84-07857) for partial support of this work.

**Registry No.** $SrH^+$, 41336-18-9; $YH^+$, 101200-09-3; $ZrH^+$, 101200-10-6; $MoH^+$, 101200-12-8; $NbH^+$, 101200-11-7; $TcH^+$, 106520-06-3; $RuH^+$, 90624-36-5; $RhH^+$, 90624-38-7; $PdH^+$, 85625-94-1; $CdH^+$, 41411-12-5.

# Theoretical Studies of Transition-Metal Methyl Ions, $MCH_3^+$ (M = Sc, Cr, Mn, Zn, Y, Mo, Tc, Pd, Cd)

**J. Bruce Schilling, William A. Goddard III,* and J. L. Beauchamp**

*Contribution No. 7553 from the Arthur Amos Noyes Laboratory of Chemical Physics, California Institute of Technology, Pasadena, California 91125.* *Received February 13, 1987*

**Abstract:** Selected transition-metal methyl cations have been studied by using ab initio generalized valence bond and configuration interaction methods. We present equilibrium geometries and bond dissociation energies and analyze the character of the wave function for the ground-state $MCH_3^+$ species. The present calculations are compared with previous studies of the corresponding $MH^+$ molecules. $MCH_3^+$ is similar to $MH^+$ from the standpoint of orbital hybridization, electron transfer, bond orbital overlap, and bond dissociation energy. Thus, we find bond energy differences $D(M^+–CH_3) - D(M^+–H)$, ranging from −3.6 kcal/mol for M = Mo to +6.0 kcal/mol for M = Zn, whereas the total bond energy is calculated to range from 24 to 60 kcal/mol. Experimental estimates suggest that $D(M^+–CH_3)$ is, on the average, about 6 kcal/mol larger than $D(M^+–H)$.

## I. Introduction

Bond dissociation energies are extremely important in chemistry for use in designing syntheses, predicting stable molecular structures, and predicting and analyzing reaction mechanisms and products. Although a large number of bond energies have been determined for organic compounds, relatively few are known quantitatively for organometallic compounds.[1-6] Even for these few, many of the bond energies are known only as averages of several metal–ligand bonds rather than as a bond energy for a particular metal–ligand bond. Recently, there have been a number of experimental determinations of bond energies for neutral[7,8] and

(1) Conner, J. A. *Top. Curr. Chem.* **1979**, *71*, 71.
(2) (a) Skinner, H. A. *Adv. Organomet. Chem.* **1964**, *2*, 49. (b) Skinner, H. A. *J. Chem. Thermodyn.* **1964**, *10*, 309.
(3) Gaydon, A. G. *Dissociation Energies and Spectra of Diatomic Molecules*; Chapman and Hall, London, 1968.
(4) Huber, K. P.; Herzberg, G. *Molecular Spectra and Molecular Structure. IV. Constants of Diatomic Molecules*; Van Nostrand Reinhold; New York, 1979.
(5) (a) Halpern, J. *Acc. Chem. Res.* **1982**, *15*, 238. (b) Halpern, J. *Inorg. Chim. Acta* **1985**, *100*, 41.
(6) (a) Yoneda, G.; Blake, D. M. *J. Organomet. Chem.* **1980**, *190*, C71. (b) Yoneda, G.; Blake, D. M. *Inorg. Chem.* **1981**, *20*, 67.
(7) Sallans, L.; Kelley, R. L.; Squires, R. R.; Freiser, B. S. *J. Am. Chem. Soc.* **1986**, *107*, 4379.

0002-7863/87/1509-5573$01.50/0 

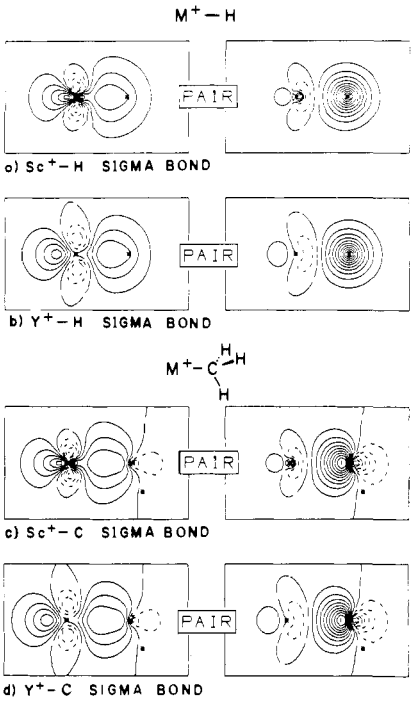


**Figure 1.** (a) GVB orbitals for $ScH^+$. The $Sc^+$–H bond length is 1.810 Å, and the metal orbital hybridization is 46.2% s, 13.5% p, and 40.3% d. (b) GVB orbitals for $YH^+$. The $Y^+$–H bond length is 1.892 Å, and the metal orbital hybridization is 31.9% s, 10.2% p, and 57.9% d. (c) GVB orbitals for the metal–carbon bond in $ScCH_3^+$ with a metal–carbon bond length of 2.233 Å and a metal–carbon-hydrogen angle of 111.0°. The orbital hybridizations are, for $Sc^+$, 45.7% s, 8.1% p, and 46.2% d, and, for C, 28.5% s, 71.3% p, and 0.2% d. (d) GVB orbitals for $YCH_3^+$ with a metal–carbon bond length of 2.298 Å and an $M^+$–C–H angle of 110.9°. The orbital hybridizations are, for $Y^+$, 25.5% s, 6.8% p, and 67.7% d, and, for C, 27.5% s, 72.3% p, and 0.2% d. For the orbital plots in this and the other figures positive contours are solid, negative contours are dotted, nodal lines are shown by long dashes, the atomic nuclei are indicated by asterisks, and the spacing between contours is 0.05 au.

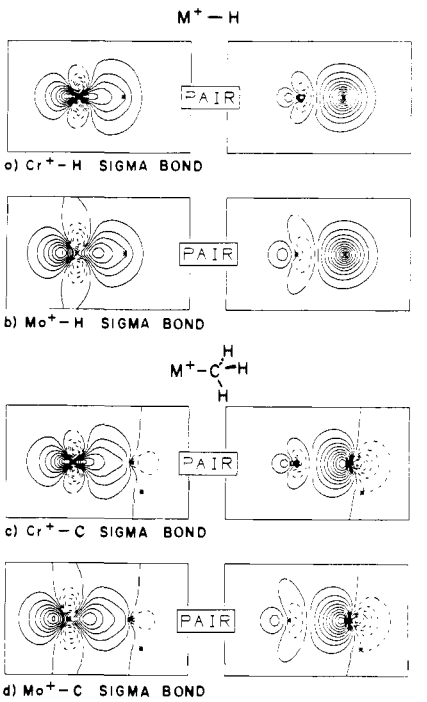


**Figure 2.** (a) GVB orbitals for $CrH^+$. The $Cr^+$–H bond length is 1.602 Å, and the metal orbital hybridization is 40.6% s, 12.5% p, and 46.9% d. (b) GVB orbitals for $MoH^+$. The $Mo^+$–H bond length is 1.708 Å, and the $Mo^+$ orbital hybridization is 19.7% s, 7.0% p, and 73.3% d. (c) GVB orbitals for the metal–carbon bond in $CrCH_3^+$ with a metal–carbon bond length of 2.074 Å and a metal–carbon–hydrogen angle of 108.4°. The orbital hybridizations are, for $Cr^+$, 41.9% s, 9.6% p, and 48.5% d, and for C, 15.3% s, 84.2% p, and 0.5% d. (d) GVB orbitals for $MoCH_3^+$ with a metal–carbon bond length of 2.201 Å and an $M^+$–C–H angle of 108.1°. The orbital hybridizations are, for $Mo^+$, 15.6% s, 3.3% p, and 81.1% d, and for C, 16.9% s, 82.7% p, and 0.4% d.

ionic[9-14] gas-phase metal compounds. In the field of hydrocarbon activation, the important bonds are $\sigma$ bonds formed to the metal center by hydrogen and carbon atoms of the organic species. Experiments suggest that in saturated metal systems the metal hydrogen bonds tend to be much stronger (approximately 15–25 kcal/mol) than the metal carbon bonds.[15-18] In unsaturated metal systems, however, such as bare transition-metal ions in the gas phase, metal methyl bond strengths have been found, experimentally, to be greater than or equal to those for the metal hydrides (differences of from 0 kcal/mol for $Ti^+$ to 14 kcal/mol for $Pd^+$) in all cases studied. The explanation for this difference between saturated and unsaturated metal systems is variously given as steric weakening of the metal–alkyl bonds in saturated molecules[19] or as increased charge stabilization of the metal ion by the alkyl group, as compared with a hydrogen atom, in the unsaturated ionic systems.[12]

In order to help explain the difference in $\sigma$ bonding between a metal and either carbon or hydrogen, we have performed ab initio theoretical calculations on a series of $MCH_3^+$ species for representative metals of the first or second transition metal series. The metal ions used were chosen because they offer a wide variety of metal bond orbital sizes and hybridizations (from almost totally s bonding for $Zn^+$ and $Cd^+$ to d bonding with $Pd^+$). These results are compared with similar calculations on the metal hydrides.[20]

## II. Results and Discussion

**Bonding in the Metal Methyl Ions.** The bond between a transition-metal and the methyl radical can be visualized as spin pairing of an electron in a metal $\sigma$ orbital (a hybrid containing s, $d_{z^2}$, and $p_z$ character) with the unpaired electron of $CH_3$ (in a carbon hybrid orbital containing s and $p_z$ character). The interaction of the metal nonbonding electrons in the metal methyls was found to be very similar to that seen for the metal hydride ions, and we considered the electric state corresponding to the ground state of $MH^+$. Under $C_{3v}$ symmetry, the metal s and $d_{z^2}$ orbitals are of $a_1$ symmetry while the $d_{xy}$, $d_{x^2-y^2}$, $d_{xz}$, and $d_{yz}$ orbitals are of e symmetry. The hydrides of the metal ions in this study are all of $\Sigma^+$ symmetry (except $ScH^+$, which is $\Pi$), and the

(8) Tolbert, M. A.; Beauchamp, J. L. *J. Phys. Chem.* **1986**, *90*, 5015.
(9) (a) Hettich, R. L.; Freiser, B. S. *J. Am. Chem. Soc.* **1986**, *108*, 2537. (b) Hettich, R. L.; Jackson, T. C.; Stanko, E. M.; Freiser, B. S. *J. Am. Chem. Soc.* **1986**, *108*, 5086.
(10) (a) Armentrout, P. B.; Halle, L. F.; Beauchamp, J. L. *J. Chem. Phys.* **1982**, *76*, 2449. (b) Stevens, A. E.; Beauchamp, J. L. *Chem. Phys. Lett.* **1981**, *78*, 291.
(11) Armentrout, P. B.; Halle, L. F.; Beauchamp, J. L. *J. Am. Chem. Soc.* **1981**, *103*, 6501.
(12) Mandich, M. L.; Halle, L. F.; Beauchamp, J. L. *J. Am. Chem. Soc.* **1984**, *106*, 4403.
(13) (a) Elkind, J. L.; Armentrout, P. B. *Inorg. Chem.* **1986**, *25*, 1078. (b) Elkind, J. L.; Armentrout, P. B. *J. Am. Chem. Soc.* **1986**, *108*, 2765. (c) Elkind, J. L.; Armentrout, P. B. *J. Phys. Chem.* **1986**, *90*, 5736. (d) Elkind, J. L.; Armentrout, P. B. *J. Phys. Chem.* **1986**, *90*, 6576.
(14) (a) Georgiadis, R.; Armentrout, P. B. *J. Am. Chem. Soc.* **1986**, *108*, 2119. (b) Aristov, N.; Armentrout, P. B. *J. Am. Chem. Soc.* **1986**, *108*, 1806. (c) Elkind, J. L.; Aristov, N.; Georgiadis, R.; Sunderlin, L.; Armentrout, P. B., to be submitted for publication.
(15) Dias, A. R.; Salema, M. S.; Simões, J. A. M. *J. Organomet. Chem.* **1981**, *222*, 69.
(16) Conner, J. A.; Zafaroni-Moattar, M. T.; Bickerton, J.; El Saied, N. I.; Suradi, S.; Carson, R.; Al Takhin, G.; Skinner, H. A. *Organometallics* **1982**, *1*, 1166.
(17) Bruno, J. W.; Marks, T. J.; Morss, L. R. *J. Am. Chem. Soc.* **1983**, *105*, 6824.
(18) Simões, J. A. M.; Beauchamp, J. L., review submitted for publication.
(19) See, for example; Ng, F. T. T.; Rempel, G. L.; Halpern, J. *Inorg. Chim. Acta* **1983**, *77*, L165.
(20) (a) Schilling, J. B.; Goddard, W. A., III; Beauchamp, J. L. *J. Am. Chem. Soc.* **1986**, *108*, 582. (b) Schilling, J. B.; Goddard, W. A., III; Beauchamp, J. L., submitted for publication. (c) Schilling, J. B.; Goddard, W. A., III; Beauchamp, J. L., submitted for publication.

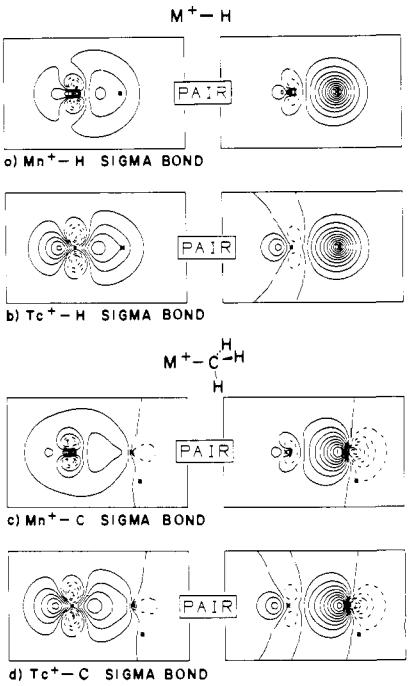


**Figure 3.** (a) GVB orbitals for $MnH^+$. The $Mn^+$–H bond length is 1.702 Å, and the metal orbital hybridization is 76.3% s, 12.5% p, and 11.3% d. (b) GVB orbitals for $TcH^+$. The $Tc^+$–H bond length is 1.719 Å, and the $Tc^+$ orbital hybridization is 40.5% s, 7.0% p, and 52.5% d. (c) GVB orbitals for the metal–carbon bond in $MnCH_3^+$ with a metal–carbon bond length of 2.241 Å and a metal–carbon–hydrogen angle of 105.5°. The orbital hybridizations are, for $Mn^+$, 86.5% s, 6.2% p, and 7.3% d, and for C, 11.1% s, 88.5% p, and 0.4% d. (d) GVB orbitals for $TcCH_3^+$ with a metal–carbon bond length of 2.209 Å and an $M^+$–C–H angle of 107.7°. The orbital hybridizations are, for $Tc^+$, 40.2% s, 3.0% p, and 81.1% d, and for C, 21.4% s, 78.1% p, and 0.5% d.

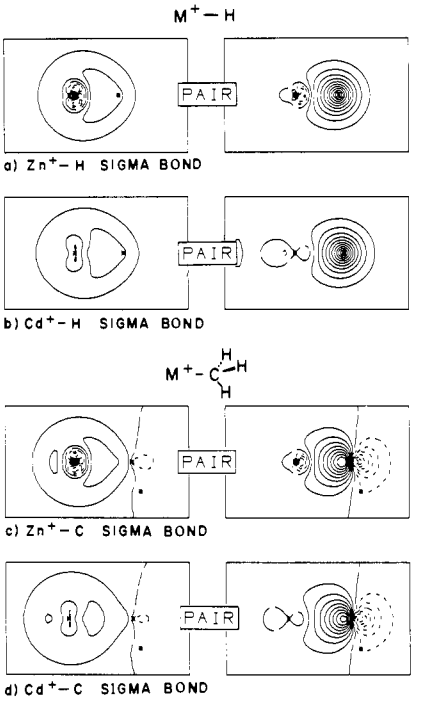


**Figure 4.** (a) GVB orbitals for $ZnH^+$. The $Zn^+$–H bond length is 1.545 Å, and the metal orbital hybridization is 90.7% s, 8.9% p, and 0.4% d. (b) GVB orbitals for $CdH^+$. The $Cd^+$–H bond length is 1.709 Å, and the $Cd^+$ orbital hybridization is 90.4% s, 9.2% p, and 0.4% d. (c) GVB orbitals for the metal–carbon bond in $ZnCH_3^+$ with a metal–carbon bond length of 2.020 Å and a metal–carbon–hydrogen angle of 106.3°. The orbital hybridizations are, for $Zn^+$, 94.8% s, 4.7% p, and 0.5% d, and for C, 12.6% s, 86.9% p, and 0.5% d. (d) GVB orbitals for $CdCH_3^+$ with a metal–carbon bond length of 2.275 Å and an $M^+$–C–H angle of 104.5°. The orbital hybridizations are, for $Cd^+$, 95.6% s, 4.0% p, and 0.4% d, and for C, 9.9% s, 89.6% p, and 0.5% d.

corresponding methyls have $A_1$ symmetry (E symmetry for $ScCH_3^+$).

Traditional oxidation state formalism describes the metal methyl species in terms of $M^{2+}$ interacting with $CH_3^-$. However, a series[21,22] of generalized valence bond calculations suggests the alternative (GVB) formalism where one starts with every ligand as neutral and bonds this ligand to the ground atomic configuration for the metal in the appropriate charge state of the metal (+1 in this case). This covalent view of the bonding to alkyl, aryl, and hydride ligands is supported by the ab initio GVB calculations. Thus, for $M^+(CH_3)$, we find a charge transfer of $-0.26$ e$^-$ (Pd) to $+0.33$ e$^-$ (Sc) from the $M^+$ to the neutral $CH_3$. The GVB bond orbitals (each with *one* electron) for various $M^+$–R species are shown in Figures 1–5. In each case the two GVB orbitals are localized with one on each of the two atoms. Each figure depicts the bond orbitals from both $MCH_3^+$ and $MH^+$ for the corresponding first- and second-row metals. The C–H orbitals for all species are essentially the same and are shown for only $PdCH_3^+$ (Figure 5).

**Geometries.** The theoretically determined metal methyl geometries are given in Table I. The C–H bond lengths have been held at the value in $CH_4$,[23] 1.094 Å, and we constrained the metal methyl ions to have $C_{3v}$ symmetry (the coordinate system is chosen with the carbon atom at the origin and the metal ion along the positive $z$ axis). Figure 6 shows potential curves for $MnH^+$ and $MnCH_3^+$ for motion of the H or $CH_3$ group with respect to the metal ion. The geometry of the $CH_3$ group is kept fixed in a

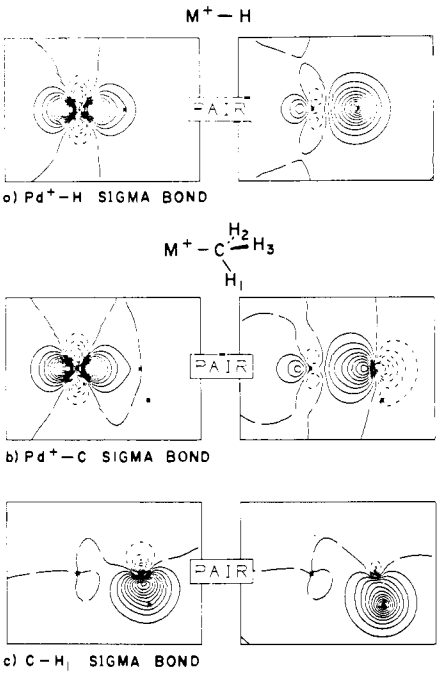


**Figure 5.** (a) GVB orbitals for $PdH^+$. The $Pd^+$–H bond length is 1.512 Å, and the metal orbital hybridization is 5.1% s, 2.1% p, and 92.8% d. (b) GVB orbitals for the metal–carbon bond in $PdCH_3^+$ with a metal–carbon bond length of 2.123 Å and an $M^+$–C–H angle of 103.5°. The orbital hybridizations are, for $Pd^+$, 4.4% s, 1.9% p, and 93.7% d, and for C, 5.3% s, 93.5% p, and 1.2% d. (c) GVB orbitals for the C–H bond in $PdCH_3^+$ with a C–H bond length of 1.094 Å.

(21) See, for example: (a) Rappé, A. K.; Goddard, W. A., III *J. Am. Chem. Soc.* **1977**, *99*, 3966. (b) Rappé, A. K.; Goddard, W. A., III, In *Potential Energy Surfaces and Dynamics Calculations*; Truhlar, D. G., Ed.; Plenum: New York, 1981. (c) Steigerwald, M. L. Ph.D. Thesis, California Institute of Technology, 1983. (d) Carter, E. A.; Goddard, W. A., III *J. Am. Chem. Soc.* **1984**, *88*, 1485.

(22) Carter, E. A.; Goddard, W. A., III *J. Am. Chem. Soc.* **1986**, *108*, 2180.

(23) Herzberg, G. *Molecular Spectra and Molecular Structure. III. Electronic Spectra of Polyatomic Molecules*; Van Nostrand Reinhold: New York, 1966.

**Table I.** Properties of Ground-State $MH^+$ and $MCH_3^+$

| molecule | state | geometry[a] $R_e(M^+-X)$, Å | geometry[a] $\angle(M^+-C-H)$, deg | force constant M–R,[b] h/Å² | force constant M–C–H,[c] mh/Å² | overlap[d] | charge transfer to ligand[d] | hybridization[d] $M^+$[e] % s | $M^+$[e] % p | $M^+$[e] % d | C[f] % s | C[f] % p | C[f] % d |
|---|---|---|---|---|---|---|---|---|---|---|---|---|---|
| $ScH^+$ | $^2\Delta$ | 1.810 | | 0.3571 | | 0.763 | 0.225 | 46.2 | 13.5 | 40.3 | | | |
| $ScCH_3^+$ | $^2E$ | 2.233 | 111.0 | 0.3239 | 0.2194 | 0.765 | 0.333 | 45.7 | 8.1 | 46.2 | 28.5 | 71.3 | 0.2 |
| $CrH^+$ | $^5\Sigma^+$ | 1.602 | | 0.4448 | | 0.734 | 0.066 | 40.6 | 12.5 | 46.9 | | | |
| $CrCH_3^+$ | $^5A_1$ | 2.074 | 103.4 | 0.3547 | 0.1866 | 0.708 | 0.041 | 41.9 | 9.6 | 48.5 | 15.3 | 84.2 | 0.5 |
| $MnH^+$ | $^6\Sigma^+$ | 1.702 | | 0.3321 | | 0.718 | 0.079 | 76.3 | 12.5 | 11.3 | | | |
| $MnCH_3^+$ | $^6A_1$ | 2.188 | 106.1 | 0.1539 | 0.1807 | 0.662 | 0.014 | 84.7 | 6.7 | 8.6 | 12.8 | 86.8 | 0.4 |
| $ZnH^+$ | $^1\Sigma^+$ | 1.545 | | 0.4713 | | 0.690 | 0.069 | 90.7 | 8.9 | 0.4 | | | |
| $ZnCH_3^+$ | $^1A_1$ | 2.020 | 106.3 | 0.3718 | 0.2038 | 0.647 | 0.020 | 94.8 | 4.7 | 0.5 | 12.6 | 86.9 | 0.5 |
| $YH^+$ | $^2\Sigma^+$ | 1.892 | | 0.3645 | | 0.760 | 0.253 | 21.9 | 10.2 | 57.9 | | | |
| $YCH_3^+$ | $^2A_1$ | 2.298 | 110.9 | 0.3673 | 0.2110 | 0.762 | 0.288 | 25.5 | 6.8 | 67.7 | 27.5 | 72.3 | 0.2 |
| $MoH^+$ | $^5\Sigma^+$ | 1.708 | | 0.4530 | | 0.703 | 0.088 | 19.7 | 7.0 | 73.3 | | | |
| $MoCH_3^+$ | $^5A_1$ | 2.201 | 108.1 | 0.3306 | 0.2089 | 0.663 | 0.114 | 15.6 | 3.3 | 81.1 | 16.9 | 82.7 | 0.4 |
| $TcH^+$ | $^6\Sigma^+$ | 1.719 | | 0.4099 | | 0.752 | 0.107 | 40.5 | 7.0 | 52.5 | | | |
| $TcCH_3^+$ | $^6A_1$ | 2.209 | 107.7 | 0.3181 | 0.2111 | 0.722 | 0.128 | 40.2 | 3.0 | 56.8 | 21.4 | 78.1 | 0.5 |
| $PdH^+$ | $^1\Sigma^+$ | 1.512 | | 0.6323 | | 0.572 | −0.115 | 5.1 | 2.1 | 92.8 | | | |
| $PdCH_3^+$ | $^1A_1$ | 2.123 | 103.5 | 0.2786 | 0.2200 | 0.475 | −0.220 | 4.4 | 1.9 | 93.7 | 5.3 | 93.5 | 1.2 |
| $CdH^+$ | $^1\Sigma^+$ | 1.709 | | 0.3912 | | 0.674 | 0.036 | 90.4 | 9.2 | 0.4 | | | |
| $CdCH_3^+$ | $^1A_1$ | 2.275 | 104.5 | 0.2371 | 0.1850 | 0.599 | −0.063 | 95.6 | 4.0 | 0.4 | 9.9 | 89.6 | 0.5 |

[a] The C–H bond length is set at 1.094 Å as in $CH_4$. [b] M–R stretch (hartrees/Å²). In $MCH_3^+$, the $CH_3$ geometry is held fixed. Multiply by 4.359 to obtain mdyne/Å and 627.5 to obtain (kcal/mol)/Å². [c] M–C–H symmetric bend (umbrella mode) (millihartrees/degree²). Multiply by 0.6275 to obtain (kcal/mol)/degree² or by $2.060 \times 10^3$ to obtain (kcal/mol)/radian.[2] [d] These properties are from the GVB–PP wave function. [e] Hybridization for the bonding orbital on $M^+$. [f] Hybridization of the carbon orbital used for bonding to $M^+$.

tetrahedral arrangement so that dissociation is to a pyramidal methyl structure rather than the ground-state planar geometry. Curves are shown for both the GVB-RCI(1/2) and RCI(1/2)×[$D_\sigma + S_{M^+,val}$] levels of calculation. The geometry found by using the latter calculation level involves an $Mn^+$–C distance of 2.124 Å and an $Mn^+$–C–H angle of 107.3° (compared to 2.188 Å and 106.1° for the GVB-RCI(1/2) calculations). The bond thus shows the normal contraction with higher levels of electron correlation (a change of 0.064 Å), and the angle opens up by about one degree. Similar effects are expected if this level of correlation were to be used for the other metal methyl species. The metal–carbon bond length is found to vary considerably from metal to metal, depending upon the size and hybridization of the metal orbital. The second-row metals tend to show a longer metal–carbon bond length than the first-row metals of the same column, with the difference ranging from 0.25 (Cd) to −0.04 (Tc). However, the bond lengths tend to emphasize the difference in metal orbital hybridization between the two rows more than the differences in metal orbital size, although both are important.

M–C–H angles are largest (111°) for the early metals (Sc and Y), with the most charge transfer to the ligand (0.33 and 0.29), and smallest (104°) for the metals (Pd and Cd), with charge transfer to the metal (−0.22 and −0.06) (Cr is a slight exception). The hybridization of the carbon bond orbital varies also with the charge transfer (28% s for Sc and Y and 5–10% s for Pd and Cd). Bond trends are consistent with a more tetrahedral geometry for the $CH_3$ anion and a more planar geometry for the $CH_3$ cation.

"Agostic" interactions[24] between C–H $\sigma$ bonds and metals have been shown to be important in some metal complexes. These interactions require empty metal orbitals that can interact with the doubly occupied $\sigma$ C–H orbital. We thus feel that if agostic interactions are important in the present systems, they should be seen in the early metal systems where there are the largest number of empty metal d orbitals. We have thus performed test calculations on $ScCH_3^+$. Three levels of calculation (GVB(1/2), GVB-RCI(1/2), and RCI(1/2)×[$D_\sigma + S_{M^+,val}$]) were used. Symmetry was restricted to $C_s$, and the H–C–H angles were kept fixed. The geometry was changed by changing the $Sc^+$–C–H angle in the $xz$ plane. These test calculations show the $C_{3v}$ symmetry to be lowest in energy, and we thus conclude that agostic interactions are not important in these ionic systems.

**Bond Orbital Hybridization.** We find the bonding in the metal methyl and metal hydride systems to be quite similar, with metal orbital hybridizations (Table I) generally changing only a few

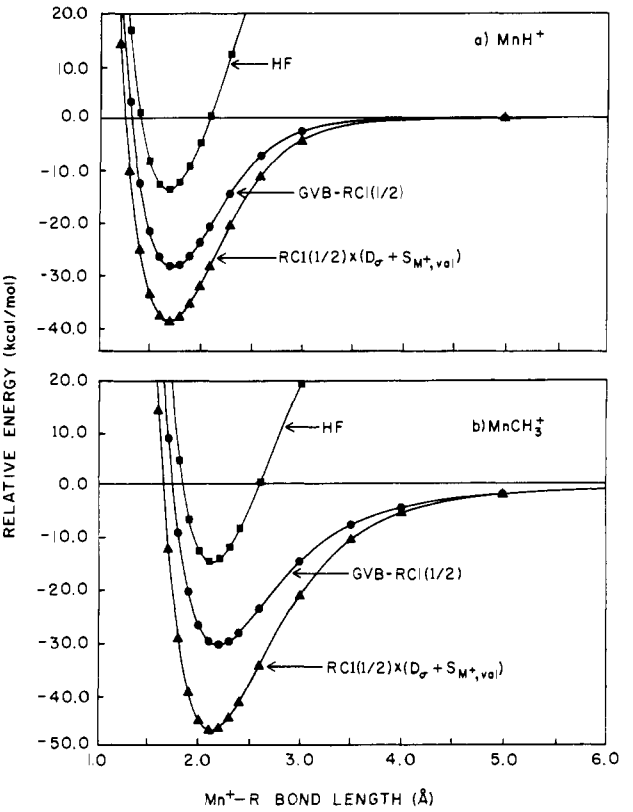


**Figure 6.** Potential energy curves showing energy vs. $M^+$–R bond distance for (a) $MnH^+$ and (b) $MnCH_3^+$. Curves are shown for both the GVB-RCI(1/2) and RCI(1/2)×[$D_\sigma + S_{M^+,val}$] levels of calculation. For $MnCH_3^+$, the H–C–H angles remain fixed at 109.5° for the entire potential curve. Thus the molecule dissociates to pyramidal $CH_3$ rather than the lowest energy planar configuration. The curves should thus not be used for obtaining values for the $Mn^+$–$CH_3$ bond dissociation energy.

percent upon replacing $CH_3$ for H. For all cases, the amount of p character in the metal–methyl bond is about half that of the hydrides. This seems to result from the directional nature of the carbon bonding orbital (sp hybrid). The metal adds in p character to polarize the bond in the direction of the ligand. With the nondirectional hydrogen 1s orbital, this effect is more important than with the directional carbon 2p orbital. For the first-row metal ions the 4s orbital is more important in bonding than the $3d_{z^2}$

(24) Brookhart, M.; Green, M. L. H. *J. Organomet. Chem.* **1983**, *250*, 395.

**Table II.** Electron Correlation Effects on the $Mn^+$–H and $Mn^+$–$CH_3$ Bond Dissociation Energies

| calculation level[a] | configs/SEFS[b] | $D_e(Mn^+–H)$, kcal/mol | configs/SEFS[b] | $D_e(Mn^+–CH_3)$, kcal/mol |
|---|---|---|---|---|
| HF | 1/1 | 13.6 | 1/1 | 8.9 |
| GVB-PP(1/2) | 2/2 | 25.9 | 2/2 | 23.2 |
| GVB-PP(4/8) | (2/2)[c] | (25.9)[c] | 16/16 | 23.0 |
| GVB-RCI(1/2) | 3/8 | 28.0 | 3/8 | 26.2 |
| GVB-RCI(4/8) | (3/8)[c] | (28.0)[c] | 80/1736 | 29.8 |
| RCI(1/2) × $D_\sigma$ | 93/333 | 37.6 | 333/1463 | 32.0 |
| RCI(1/2) × [$D_\sigma$ + $S_{M^+}$] | 168/523 | 38.7 | 563/2053 | 33.2 |
| RCI(1/2) × [$D_\sigma$ + $S_{M^+,val}$] | 168/523 | 38.7 | 726/3896 | 40.3 |

[a] See the calculational details section of the text for an explanation of the various calculations. [b] Number of configurations and spin eigenfunctions in the wave function. [c] GVB-PP(4/8) and GVB-RCI(4/8) calculations are not possible for $MnH^+$. The numbers in parentheses are thus from the comparable GVB-PP(1/2) and GVB-RCI(1/2) calculations on $MnH^+$.

orbital, while for the second-row metals the 4d orbitals are more important than the 5s. The general trend in sd hybridization is that, for metal–carbon bonds, the dominant orbital in the hybrid becomes even more dominant as the p character is decreased. The hybridization of the carbon orbital is governed by the charge transfer and the metal atomic configuration. Thus, $ScCH_3^+$ and $YCH_3^+$ with charge transfers to $CH_3$ of 0.29 and 0.33 lead to 28% s character in the C orbital (much like the $CH_3$ anion), whereas $PdCH_3^+$ and $CdCH_3^+$ with transfers of 0.22 and 0.06 *away* from $CH_3$ lead to 5 and 10% s character (much like $CH_3$ radical). The atomic character on the metal ion plays a dominant role. Thus $Zn^+$ and $Cd^+$ (both strongly $d^{10}s^1$) lead to bonds with 95% s character. Similarly, $Mn^+$ (which strongly prefers $d^5s^1$) leads to 87% s character in the bond. On the other hand, $Mo^+$ (strongly $d^5$) and $Pd^+$ (strongly $d^9$) lead to 81% and 94% d character in the bond. For $Y^+$ and $Tc^+$, the $d^{n-1}s^1$ to $d^n$ state splittings are 0.88 and 0.51 eV,[25] respectively (the $Y^+$ ground state is $^1S$ ($s^2$), 0.16 eV below the $^3D$ ($s^1d^1$) state); however, the strong d bonding in the second row leads to d character of 68% and 57% in the bonds. $Cr^+$, like $Mo^+$, is strongly $d^5$; however, loss of high-spin exchange energy and strong first-row s bonds decrease the d character to 49%. For $Sc^+$, the $d^{n-1}s^1$ to $d^n$ state splitting is only 0.6 eV and the s and d character in the bond is similar, ~46%.[25]

**Bond Energies.** We used $MnH^+$ and $MnCH_3^+$ as the prototypes for studying the effects of various levels of electron correlation on bond energy. Table II shows the bond dissociation energies for these molecules at various levels of calculation. [The generalized valence bond and configuration interaction (CI) wave functions are described in the Calculational Details of this paper.] Major points are as follows. (1) Proper dissociation: electron correlation in the bond being formed is essential for proper dissociation to fragments [cf. HF to GVB-PP(1/2)] (see Figure 6). (2) Spin coupling on the metal: some triplet character in the bond is induced by spin coupling to the $d^5$ nonbonding configuration [cf. GVB-PP(1/2) to GVB-RCI(1/2)]. This leads to a 2–3 kcal/mol increase in bond energy for both cases. (3) M–C and C–H correlations: for $MnCH_3^+$, the correlation in the three C–H bonds adjacent to the $Mn^+$–C bond is important [cf. GVB-RCI(1/2) to GVB-RCI(4/8)]. It is the instantaneous motion of the two electrons in the M–C bond simultaneously with two electrons in the C–H bond

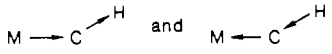


that is important, since there is no difference between GVB-PP(1/2) and GVB-PP(4/8). This is worth 3.6 kcal/mol for the $M^+$–$CH_3$ case (there is no effect in $MH^+$). (4) Full correlation of bond pair: the fully correlated bond pair (within the basis) is obtained with RCI(1/2)×$D_\sigma$. This increases the bond energy by 9.6 kcal/mol for $MH^+$ and 5.5 kcal/mol for $MCH_3^+$. This does *not* allow for instantaneous correlations in either the metal d electrons or the C–H bonds. (5) M–R and Md correlations: the RCI(1/2)×[$D_\sigma$ + $S_{M^+}$] allows for readjustment of the metal d orbitals simultaneous with correlation of the electrons in the bond pair. This increases the bond energy 1.1 kcal/mol for $M^+$–H and 1.2 kcal/mol for $M^+$–$CH_3$. (6) M–R and C–H correlations: the RCI(1/2)×[$D_\sigma$ + $S_{M^+,val}$] improves upon (5) by allowing readjustment in all valence electrons simultaneously with correlation in the M–C pair [as in (3)] leading to a 7.1 kcal/mol effect for $MCH_3^+$. (7) The M–H and M–C bond energies are very similar with M–C about 1.7 kcal/mol stronger. (8) The simplest wave function with accurate *relative* bonding energies is GVB-RCI(4/8) (only 81 spatial configurations) which leads to a 1.8 kcal/mol stronger $M^+$–C bond. The best bond energy estimates come from the RCI(1/2)×[$D_\sigma$ + $S_{M^+,val}$] calculations which involve correlation of both the C–H and M valence electrons and are equivalent to the DCCI-GEOM[20] calculations used for geometry optimization and state splitting calculations on the $MH^+$ species. For methane this calculation level[26] leads to, $D_e(H–CH_3)$ = 110.5 kcal/mol, only 1.7 kcal/mol below the experimental value of $D_e$ = 112.2 ± 0.5 kcal/mol. This calculation level was used for all bond energy discussions of $MH^+$ and $MCH_3^+$.

Table III contains the calculated total energies for several calculation levels for $MCH_3^+$, $MH^+$, $M^+$, $CH_3$, and H (at the equilibrium geometries for the molecular species). The calculated bond dissociation energies $D_e(M^+–CH_3)$ are presented in Table IV. The bond energies cover a range 35 kcal/mol with a high of 60.7 kcal/mol for $ZnCH_3^+$ and a low of 24.1 kcal/mol for $CrCH_3^+$. As with the metal hydrides, the variation in bond dissociation energies is due to several interrelated factors. The methyl group can be thought of as having a certain "intrinsic" bond energy when bonded to pure metal s, p, or d orbitals. The "intrinsic" bond energies are then moderated by (1) the energy gained from orbital hybridization, (2) the promotion energy cost to promote the metal ion to an electronic state having the proper metal orbital for bonding to the ligand, and (3) the amount of energy lost due to loss of atomic electron exchange energy (favoring high spin) upon decoupling one metal electron from the others to form the bond.

"Intrinsic" bond energy trends for the metal hydrides[20] indicate that as one moves from left to right in a given row of transition metals, the bond energy to a metal s orbital slowly increases as the s orbital size decreases while the bond energy to a metal d orbital decreases rapidly as the d orbital size decreases. Due to the larger size of the orbitals of the second-row metals, s bonds tend to be slightly weaker and d bonds (at least toward the later metals) tend to be stronger than for the first row. The general trends are expected to be similar for the metal methyl molecules. This is partially born out by the fact that the strongest bonds are formed by very early (e.g., $Sc^+$ and $Y^+$) or very late (e.g., $Zn^+$ and $Cd^+$) metals, where the early metals use significant amounts of d character and $Zn^+$ and $Cd^+$ use almost all metal s character.

The strong bonds formed to the early metals are also due to the presence of low-lying metal electronic states allowing extensive s–d hybridization. This is complimented by the small amounts of exchange energy lost on bonding. The low bond energies for $CrCH_3^+$ and $MoCH_3^+$ (both $d^5$) are due to the large amount of exchange energy lost on bonding and by the inaccessability of the metal $^6D$ ($d^4s^1$) state, which is over 1.5 eV above the $^6S$ ($d^5$) ground state.[25]

One must be careful in comparing theoretical and experimental differences between metal–hydride and metal–methyl bond dissociation energies. The theoretical bond energies are $D_e$ values

(25) Moore, C. E. *Atomic Energy Levels*; National Bureau of Standards, Washington, D.C., 1971; Vols. I, II, and III.
(26) Carter, A. E.; Goddard, W. A., III, manuscript in preparation.

**Table III.** Total Energies for Ground-State $MCH_3^+$, $M^+$, and $CH_3$[a]

| species | state | total energy,[b] hartrees | | | | |
|---|---|---|---|---|---|---|
| | | GVB(1/2) | GVB-RCI(1/2) | GVB(4/8) | GVB-RCI(4/8) | RCI(1/2) × $[D_\sigma + S_{M^+,val}]$ |
| $ScCH_3^+$ | $^2E$ | −798.288 70 | −798.288 86 | −798.332 45 | −798.350 02 | −798.319 69 |
| $Sc^+$ | $^3D$ | −758.663 17 | −758.663 17 | −758.663 17 | −758.663 17 | −758.663 17 |
| $CrCH_3^+$ | $^5A_1$ | −1081.541 59 | −1081.546 81 | −1081.584 93 | −1081.605 58 | −1081.580 53 |
| $Cr^+$ | $^6S$ | −1141.976 41 | −1141.976 41 | −1141.976 41 | −1141.976 41 | −1141.976 41 |
| $MnCH_3^+$ | $^6A_1$ | −1187.963 60 | −1187.968 51 | −1188.007 24 | −1188.028 21 | −1188.000 24 |
| $Mn^+$ | $^7S$ | −1148.366 28 | −1148.366 28 | −1148.366 28 | −1148.366 28 | −1148.366 28 |
| $ZnCH_3^+$ | $^1A_1$ | −1815.194 27 | −1815.194 27 | −1815.238 24 | −1815.254 03 | −1815.222 84 |
| $Zn^+$ | $^2S$ | −1775.556 52 | −1775.556 52 | −1775.556 52 | −1775.556 52 | −1775.556 78 |
| $YCH_3^+$ | $^2A_1$ | −76.905 19 | −76.905 34 | −76.948 60 | −76.765 62 | −76.936 98 |
| $Y^+$[c] | $^3D$ | −37.268 55 | −37.268 55 | −37.268 55 | −37.268 55 | −37.268 55 |
| $MoCH_3^+$ | $^5A_1$ | −106.251 44 | −106.257 42 | −106.294 66 | −106.315 73 | −106.289 96 |
| $Mo^+$ | $^6S$ | −66.672 12 | −66.672 12 | −66.672 12 | −66.672 12 | −66.672 12 |
| $TcCH_3^+$ | $^6A_1$ | −118.758 63 | −118.766 12 | −118.802 29 | −118.825 49 | −118.801 24 |
| $Tc^+$ | $^7S$ | −79.163 02 | −79.163 02 | −79.163 02 | −79.163 02 | −79.163 02 |
| $PdCH_3^+$ | $^1A_1$ | −165.243 32 | −165.243 32 | −165.287 31 | −165.299 01 | −165.274 19 |
| $Pd^+$ | $^2D$ | −125.628 86 | −125.628 86 | −125.628 86 | −125.628 86 | −125.629 41 |
| $CdCH_3^+$ | $^1A_1$ | −85.918 81 | −85.918 81 | −85.963 05 | −85.977 96 | −85.947 60 |
| $Cd^+$ | $^2S$ | −46.299 16 | −46.299 16 | −46.299 16 | −46.299 16 | −46.300 65 |
| $CH_3$ | $^2A_1$ | −39.560 32 | −39.560 32 | −39.604 27 | −39.614 40 | −39.569 66 |

[a] Energies are for molecules at their equilibrium geometries. [b] For $MCH_3^+$ the total energies are for the calculation levels shown while the $M^+$ and $CH_3$ total energies are for the calculation levels to which these $MCH_3^+$ molecules dissociate (see Calculational Details of text). [c] The $^2A_1$ state of $YCH_3^+$ does not dissociate to ground state $Y^+$ ($^1S$) but to $^3D$ $Y^+$ as shown here.

**Table IV.** A Comparison of Theoretical and Experimental $MH^+$ and $MCH_3^+$ Bond Dissociation Energies[a]

| metal | theory | | | | | | experiment | | | |
|---|---|---|---|---|---|---|---|---|---|---|
| | $D_e(M^+-H)$ | | $D_e(M^+-CH_3)$ | | $\Delta D_e$[d] | | | | | |
| | RCI[b] | CI[c] | RCI[b] | CI[c] | RCI | CI | $D_{298}(M^+-H)$[e] | $D_{298}(M^+-CH_3)$[f] | $\Delta D_{298}$(EXP)[g] | $\Delta(\Delta D)$[h] |
| Sc | 47.5 | 56.6 | 45.5 | 54.5 | −2.0 | −2.1 | 56.2 ± 2.0 | 59 ± 3 | 2.8 | 4.9 |
| Cr | 11.2 | 25.3 | 9.2 | 24.1 | −2.0 | −1.2 | 27.7 ± 2.0 | 30 ± 5 | 2.3 | 3.5 |
| Mn | 28.0 | 38.7 | 29.8 | 40.3 | 1.8 | 1.7 | 48.4 ± 1.4 | 51 ± 2 | 2.6 | 0.9 |
| Zn | 44.4 | 54.7 | 52.2 | 60.7 | 8.8 | 6.0 | 57.7[i] | 70.6 ± 3.2 | 12.9 | 6.9 |
| Y | 49.4 | 58.8 | 48.2 | 58.3 | −1.2 | −0.5 | 59 ± 3 | 64 ± 7 | 5.0 | 5.5 |
| Mo | 22.2 | 33.8 | 18.3 | 30.2 | −3.9 | −3.6 | 42 ± 3 | | | |
| Tc | 32.0 | 44.4 | 30.2 | 43.0 | −1.8 | −1.4 | | | | |
| Pd | 30.5 | 45.3 | 35.0 | 47.1 | 4.5 | 1.8 | 45 ± 3[j] | 59 ± 5[j] | 14.0 | 12.2 |
| Cd | 36.3 | 45.6 | 40.4 | 48.5 | 4.1 | 3.8 | | | | |

[a] All values are given in kcal/mol. [b] RCI represents GVB-RCI(1/2) for $MH^+$ and GVB-RCI(4/8) for $MCH_3^+$. [c] CI represents the RCI(1/2) × $[D_\sigma + S_{M^+,val}]$ calculation. [d] $\Delta D_e$ is defined as $D_e(M^+-CH_3) - D_e(M^+-H)$ for the two levels of calculation. [e] From ref 13, unless otherwise noted. The values in the reference are given as $D_0$ and have been changed to $D_{298}$ by addition of 0.9 kcal/mol. [f] From ref 14, unless otherwise noted. [g] $\Delta D_{298}$ is defined as $D_{298}(M^+-CH_3) - D_{298}(M^+-H)$ for the experimental values. [h] $\Delta(\Delta D) = \Delta D_{298}(EXP) - \Delta D_e(CI)$. [i] From ref 4. [j] From ref 12.

while the experimental values are generally determined at ~298 K. Thus we must estimate the difference between $D_e$ and $D_{298}$ for $MH^+$ and $MCH_3^+$. Assuming an ideal gas with only translational and rotational degrees of freedom active, the differences in bond dissociation energies between 0 and 298 K are $D_0(M^+-H) = D_{298}(M^+-H) - 0.9$ kcal/mol and $D_0(M^+-CH_3) = D_{298}(M^+-CH_3) - 1.5$ kcal/mol. Our calculations yield the metal–hydrogen or metal–carbon vibrational force constants and also the $CH_3$ umbrella mode force constant (see Table I), but we did not allow other metal methyl motions in our calculations. The average zero point energy for the hydrides of the nine metal ions in this study is $D_e - D_0 = 2.5$ kcal/mol. Frequencies have been measured experimentally for $CuCH_3$,[27] and $ZnCH_3$[28] (in a $BH_4^-ZnCH_3^+$ salt). $CH_3Br$ and $CH_3I$[23] should also give good estimates for vibrational frequencies. Zero-point energies for the four species vary from 21.2 to 22.6 kcal/mol with an average of 22.1 kcal/mol. The experimentally determined vibrational frequencies for the methyl radical[29] lead to a zero-point energy of 18.2 kcal/mol. For the $MCH_3^+$ species, the zero-point energy leads to $D_e - D_0 \approx 3.9$ kcal/mol. Thus, for $MH^+$, $D_{298} = D_e - 1.6$, and for $MCH_3^+$, $D_{298} = D_e - 2.4$. Thus $D_{298}(M^+-C) - D_{298}(M^+-H) = D_e(M^+-C) - D_e(M^+-H) - 0.8$.

By and large, the theory leads to similar $M^+-H$ and $M^+-C$ bond energies (average difference: 0.4 kcal/mol in favor of $M^+-C$). The values range from 3.6 kcal/mol weaker ($MoCH_3^+$) to 6.0 kcal/mol stronger ($ZnCH_3^+$). On the other hand, experimental studies[13,14,30] find metal methyl ion bond dissociation energies to be stronger than that for the corresponding metal hydrides by about 6 kcal/mol on the average. Indeed, with use of bond dissociation energies for $Sc^+-Mn^+$ from the most recent ion beam studies,[13,14] the average difference in metal–methyl and metal–hydrogen bond strengths is 1.7 kcal/mol. For $Fe^+$, $Co^+$, $Ni^+$, and $Zn^+$ the average experimental difference is 9.9 kcal/mol. Less is known experimentally about the second-row transition metals. $YCH_3^+$ and $RhCH_3^+$ bond energies[12,14] are found to be 5 kcal/mol stronger than the respective hydrides, while $RuCH_3^+$ and $PdCH_3^+$ are reported 13 and 14 kcal/mol stronger.[12]

Table IV compares the theoretical and experimental bond dissociation energies for various $MH^+$ and $MCH_3^+$. It should be pointed out that the CI values for $D_e(M^+-H)$ are for the RCI(1/2)×$[D_\sigma + S_{M^+,val}]$ (DCCI-GEOM calculations of ref 20) which correspond to the calculations on $MCH_3^+$ and not to the highest level of calculation performed on the metal hydrides (DCCI calculations of ref 20). The numbers presented here will thus be slightly different than the bond dissociation energies published elseware.[20] It should also be emphasized that there remain sig-

(27) Adams, D. M. *Metal-ligand and Related Vibrations: A Critical Survey of the Infrared and Raman Spectra of Metallic and Organometallic Compounds*; Edward Arnold Ltd.: London, 1967.

(28) Nibler, J. W.; Cook, T. H. *J. Chem. Phys.* **1973**, *58*, 1596.

(29) (a) Holt, P. L.; McCurdy, K. E.; Weisman, R. B.; Adams, J. S.; Engel, P. S. *J. Chem. Phys.* **1984**, *81*, 3349. (b) Tan, L. Y.; Winer, A. M.; Pimentel, G. C. *J. Chem. Phys.* **1972**, *57*, 4028. (c) Amano, T.; Bernath, P. F.; Yamada, C.; Endo, Y.; Hirota, E. *J. Chem. Phys.* **1982**, *77*, 5284. (d) Snelson, A. *J. Phys. Chem.* **1970**, *74*, 537.

(30) Tolbert, M. A.; Beauchamp, J. L. *J. Am. Chem. Soc.* **1984**, *106*, 8117.

nificant uncertainties in the experimental numbers. Most of the $M^+ + H_2$ reactions used for determining $D(M^+-H)$ have been extensively reevaluated to determine the role of excited-state metal ions in the beam.[13] This had led to decreases in the experimental $M^+-H$ bond energies by up to 10 kcal/mol (in the case of $FeH^+$). Similar reevaluation has not been made for most of the metal methyl experiments (the values for $VCH_3^+$ and $ZnCH_3^+$ are probably the best) so that the experimental bond energies may yet be closer to the metal–hydride bond energies (and closer to the theoretical values).

For saturated metal systems, the few molecules where directly comparable bond energies for $M-CH_3$ and M–H bonds have been determined, all lead to much stronger metal–hydrogen bonds, with an average difference of 18 kcal/mol. The systems (differences in bond dissociation energies) are $Cp_2MoR_2$ (23 kcal/mol),[15] $Cp_2WR_2$ (23 kcal/mol),[15] $Cp^*_2ThR_2$ (13 kcal/mol),[17] and $Mn(CO)_5R$ (15 kcal/mol)[16] where Cp is the cyclopentadienyl ligand, Cp* is the pentamethylcyclopentadienyl ligand, and R is $CH_3$ or H. Bond energies to larger alkyl fragments have generally been found to be quite weak (on the order of 20 kcal/mol in some Co systems).[5] In general, the low M–C bond energies are attributed to steric factors, altough it could also be due partly to the relaxation energies of the alkyl radical (which is absent in the M–H bond breaking process).

Several theoretical calculations comparing M–H and $M-CH_3$ bonds in neutral metal systems have also been carried out. Low and Goddard[31] studied $PdR_2$ and $PtR_2$ (R = H, $CH_3$), finding average bond energy differences of 14.2 and 15.7 kcal/mol for Pd and Pt, respectively (M–H stronger than M–C), whereas for $(PH_3)_2PdR_2$ and $(PH_3)_2PtR_2$ they find differences of 17.3 and 18.7 kcal/mol. These calculations did not correlate the CH bonds (although they did correlate the d orbitals) and hence may be biased against the M–C bonds. Carter and Goodard[26] studied several ClRu–R systems, which yielded Ru–H and $Ru-CH_3$ bond energies that are within 0.2 kcal/mol of each other when electron correlation is included between the M–C and C–H bond electrons, while the $Ru-CH_3$ bond energy is weaker than the Ru–H bond energy by 13 kcal/mol when this electron correlation is not included. Calculations on $Cr^+-R$ *without* correlation of the C–H electrons[32] lead to a chromium–methyl bond energy which is 7.1 kcal/mol lower than the chromium–hydrogen bond energy while the present study (including this correlation) gives a bond energy difference of only 1.2 kcal/mol. Thus, for bond energy purposes, correlation of the C–H electrons with the electrons in the bond being broken is very important (5–13 kcal/mol). Summarizing, the calculations suggest that the M–C and M–H bonds are very similar in systems with little or no steric hindrance.

For the metal ion systems, the "increased" strength of the metal–carbon bond is usually explained as due to stabilization of the ionic charge by either resonance effects

$$M^+-CH_3 \leftrightarrow M-CH_3^+$$

or through an ion-induced dipole interaction. The latter effect can be estimated by using

$$V(r) = \frac{-e^2\alpha}{2R^4} = \frac{166\alpha}{R_0^4} \text{ kcal/mol}$$

where $R_0$ is the internuclear separation in Å, $\alpha$ is the ligand polarizability in Å$^3$, and $e$ is the unit charge of the electron.[33] Average values of $\alpha$ for H and $CH_3$ are 0.4 and 1.95 Å$^3$, respectively.[33,34] Although this equation does not take into account covalent bonding interactions or electron–electron repulsion, it does give some idea as to the stability that could be imparted due to dipolar effects. Setting $R_0$ equal to the calculated bond lengths for the species, the average difference in $V(r)$ for $M^+-H$ and $M^+-CH_3$ is only 5.5 kcal/mol. Thus it is possible that ion-induced dipole effects could play a small part in the bonding. However, the charge transfer from the metal to the ligand for $MH^+$ and $MCH_3^+$ is quite similar, and differences in charge transfer do not correlate with increased metal–methyl bond energies.

## III. Summary

We report ab initio theoretical calculations on $MCH_3^+$ for nine transition-metal systems representing a variety of bonding conditions. In all instances the metal–methyl bonds are very similar to the $\sigma$ bonds found in $MH^+$ systems. This similarity includes bond orbital overlaps, charge transfer, and metal orbital hybridization. A comparison of $M^+-C$ and $M^+-H$ theoretical bond energies also shows that the two types of $\sigma$ bond are very similar (the average difference for the nine metal systems being ~0.4 kcal/mol).

## IV. Calculational Details

**Basis Sets.** The same metal basis sets have been used as in the previously published metal hydride calculations. The first-row metals are described by the all electron valence double-$\zeta$ (VDZ) basis sets of Rappé and Goddard[35] (13s,10p,5d/5s,4p,2d). The second-row metals, except Cd, are described by using the effective potential basis sets of Hay and Wadt,[36] which treat the 4s, 4p, 5s, 4d electrons explicitly (5s,5p,4d/4s,4p,3d). The Cd basis is also a Hay and Wadt effective potential basis,[37] however, the 4s and 4p electrons are included in the effective core potential (3s,3p,4d/3s,3p,3d). The Dunning/Huzinaga[38] VDZ bases were used for C (9s,5p/3s,2p) and H (4s/2s), where $\zeta$ = 1.2 for H bonded to C and $\zeta$ = 1.0 for H bonded to M. One set of d polarization functions is included on C ($\zeta$ = 0.64).[39]

**Geometry Optimization.** The metal methyl ion geometries were optimized at the GVB-RCI(1/2) level of calculation (generalized valence bond restricted configuration interaction). The geometry was optimized as follows. The orientation around the carbon was initially fixed ($C_{3v}$ symmetry) by using tetrahedral bond angles (109.5°) and the methane bond length (1.094 Å). The metal–carbon bond length was then optimized. With this new $M^+-C$ bond length, the optimum $M^+-C-H$ angle was found. If the bond angle changed by greater than 5°, a second bond length optimization was performed. The C–H bond distance remained fixed throughout the geometry optimization.

**Wave Functions.** Bond dissociation energies were calculated at the GVB-PP(1/2), GVB-PP(4/8), GVB-RCI(1/2), GVB-RCI(4/8), RCI(1/2) × $D_\sigma$, RCI(1/2)×[$D_\sigma$ + $S_{M^+}$], and RCI(1/2)×[$D_\sigma$ + $S_{M^+,val}$] levels of calculation. A comparison of the bond energies for $MnH^+$ and $MnCH_3^+$ at the various levels is presented in Table II. The CI bond energies presented in Table IV for all species is at the RCI(1/2)×[$D_\sigma$ + $S_{M^+,val}$] level, which allows the molecules to dissociate smoothly to the metal ion and the ground state of the ligand. All molecules dissociate to the ground electronic state of the metal ion except for $YCH_3^+$ which dissociates to $CH_3$ and $^3D$ $Y^+$. In this case the bond energy is determined by subtracting the experimental state splitting between the $^3D$ and $^1S$ states from the diabatic dissociation energy. A description of the various SCF and configuration interaction calculations follows:

(1) GVB-PP(1/2) and GVB-PP(4/8). In the perfect pairing (PP) approach to GVB, each bond pair is assumed to have pure singlet spin pairing (as in a simple VB spin function), but all orbitals are optimized. For N bond pairs, this leads to $2^N$ configurations.

(2) GVB-RCI(1/2) and GVB-RCI(4/8). Restricted CI calculations allow the two electrons of each GVB bond pair to occupy the two orbitals in all three possible ways, allowing either covalent

(31) (a) Low, J. J.; Goddard, W. A., III *J. Am. Chem. Soc.* **1984**, *106*, 6928. (b) Low, J. J.; Goddard, W. A., III *Organometallics* **1986**, *5*, 609. (c) Low, J. J.; Goddard, W. A., III *J. Am. Chem. Soc.* **1986**, *108*, 6115.
(32) Alverado-Swaisgood, A. E.; Allison, J.; Harrison, J. F. *J. Phys. Chem.* **1985**, *89*, 2517.
(33) Benson, S. W. *Thermochemical Kinetics*; Wiley: New York, 1976.
(34) Hirschfelder, J. O.; Curtiss, C. F.; Bird, R. B. *Molecular Theory of Gases and Liquids*; Wiley: New York, 1954.
(35) (a) Rappé, A. K.; Goddard, W. A., III, to be submitted for publication. (b) Rappé, A. K.; Smedley, T. A.; Goddard, W. A., III *J. Phys. Chem.* **1981**, *85*, 260.
(36) Hay, J. P., Wadt, W. R. *J. Chem. Phys.* **1985**, *82*, 299.
(37) Hay, J. P.; Wadt, W. R. *J. Chem. Phys.* **1985**, *82*, 270.
(38) (a) Huzinaga, S. *J. Chem. Phys.* **1965**, *42*, 1293. (b) Dunning, J. H., Jr. *J. Chem. Phys.* **1970**, *43*, 2823.
(39) Bair, R. A.; Goddard, W. A., III, unpublished results.

or ionic bonding. This allows all spin couplings (different VB structures), a particularly important effect for atoms with partially filled d configurations. For a wave function with N GVB pairs, this leads to $3^N$ configurations and hence three configurations for (1/2) and 81 configurations for (4/8). These calculations are dissociation-consistent: GVB-RCI(1/2) dissociates to a Hartree–Fock (HF) description of both $M^+$ and $CH_3$; GVB-RCI(4/8) dissociates to an HF description of $M^+$ and a GVB-RCI(3/6) description of $CH_3$. For the metal hydrides the GVB-RCI(1/2) calculations dissociate to HF fragments.

(3) RCI(1/2)×$D_\sigma$. From the three RCI configurations all single and double excitations are allowed out of the metal–ligand $\sigma$ bond to all virtual orbitals. This calculation allows for all correlation between the two electrons of the bond pair. It dissociates to an HF×$S_\sigma$ description for both the metal ion and the $CH_3$ fragments (the single excitation is from the s or $d_{z^2}$ orbital on the metal, depending on which is used for bonding, and from the $p_z$ orbital on $CH_3$). Metal hydrides dissociate to an HF×$S_\sigma$ description of $M^+$ and an HF H atom.

(4) RCI(1/2)×[$D_\sigma$ + $S_{M^+}$]. To the configurations of (3) we add all those formed by starting with the RCI configurations and allowing single excitations from the metal nonbonding valence orbitals (to all occupied and virtual orbitals). This calculation dissociates to an HF calculation on the ligand and an all singles CI for the metal valence orbitals.

(5) RCI(1/2)×[$D_\sigma$ + $S_{M^+,val}$]. This calculation is similar to (4) except that the single excitations are allowed out of all valence orbitals, not just those of the metal ion. For the metal hydrides the two calculations are the same. The metal methyls dissociate to an HF×$S_{val}$ description on both fragments. This leads to an overcorrelation of the fragments in some cases (if single excitations on the metal lead to an energy lowering, e.g., $ZnCH_3^+$, $PdCH_3^+$, and $CdCH_3^+$) and hence to a calculated dissociation energy that may be slightly too low. This effect is not large and calculations by Carter and Goddard[22] on $RuCH_2$ involving a similar dissociation error show that the bond energy is underestimated by ~0.2 kcal/mol. We expect a similar error in our cases. As a test of the adequacy of this level of electron correlation, Carter and Goddard[26] performed a similar calculation breaking the C–H bond in $CH_4$. The theoretical bond dissociation energy was calculated at 110.5 kcal/mol in comparison to an experimental $D_e$ of 112.2 ± 0.5 kcal/mol. The calculated bond dissociation energy is thus only 1.7 kcal/mol lower than the experimental value, suggesting that our comparable calculations on $MCH_3^+$ species should be quite adequate.

**Acknowledgment.** We thank the National Science Foundation (Grants CHE83-18041 and CHE84-07857) for partial support of this work.

**Registry No.** $ScH^+$, 83018-00-2; $ScCH_3^+$, 93349-11-2; $CrH^+$, 75641-98-4; $CrCH_3^+$, 89612-53-3; $MnH^+$, 75641-96-2; $MnCH_3^+$, 89612-54-4; $ZnH^+$, 41336-21-4; $ZnCH_3^+$, 47936-33-4; $YH^+$, 101200-09-3; $YCH_3^+$, 109585-23-1; $MoH^+$, 101200-12-8; $MoCH_3^+$, 109585-24-2; $TcH^+$, 106520-06-3; $TcCH_3^+$, 106500-86-1; $PdH^+$, 85625-94-1; $PdCH_3^+$, 90624-40-1; $CdH^+$, 41411-12-5; $CdCH_3^+$, 106520-07-4; $Sc^+$, 14336-93-7; $Cr^+$, 14067-03-9; $Mn^+$, 14127-69-6; $Zn^+$, 15176-26-8; $Y^+$, 14782-34-4; $Mo^+$, 16727-12-1; $Tc^+$, 20205-77-0; $Pd^+$, 20561-55-1; $Cd^+$, 14445-53-5; $CH_3^\bullet$, 2229-07-4.

# Bond Energy and Other Properties of the Re–Re Quadruple Bond

**David C. Smith and William A. Goddard III***

*Contribution No. 7558 from the Arthur Amos Noyes Laboratory of Chemical Physics, California Institute of Technology, Pasadena, California 91125.* *Received February 18, 1987*

**Abstract:** Using generalized valence bond (GVB) methods designed for obtaining accurate bond energies, we predict an Re–Re quadruple bond strength of 85 ± 5 kcal/mol for $Re_2Cl_8^{2-}$. This is much less than early estimates of 370 kcal/mol and somewhat lower than estimates (124 to 150 kcal/mol) based on Birge–Sponer extrapolation but is in reasonable agreement with a recent thermochemical study (97 ± 12 kcal/mol). We obtain a rotational barrier of 3.0 kcal/mol and a singlet–triplet excitation energy of 3100 $cm^{-1}$, and we conclude that the intrinsic strength of the $\delta$ bond is 6 ± 3 kcal/mol.

Since their discovery in 1965, quadruply bonded metal dimers have provoked numerous theoretical and experimental studies. A particularly controversial issue has been the strength of the quadruple bond and, in particular, the contribution of the $\delta$ bond to the observed structure of the unbridged dimers.[1-4] We here report the results of ab initio calculations of $Re_2Cl_8^{2-}$ designed to provide accurate bond energies and torsion barriers as well as accurate shapes for the potential curves. These studies use the generalized valence bond (GVB) approach in which electron correlations are included for all eight electrons available for the quadruple bond, while solving self-consistently for all orbitals.[5,6]

We use the modified-GVB (M-GVB) approach of Goodgame and Goddard.[7] They pointed out that ab initio descriptions of multiple bonds in transition metals lead to substantial errors in the bond energy due to an inadequate treatment of the electron correlations in the ionic part of the wave function describing the bond.

$$\psi^{GVB} = \psi_{cov} + \lambda\psi_{ionic} = [\phi_l(1)\phi_r(2) + \phi_r(1)\phi_l(2)] + \lambda[\phi_l(1)\phi_l(2) + \phi_r(1)\phi_r(2)]$$

In GVB, electron correlation in the covalent part of the wave

(1) Cotton, F. A.; Walton, R. A. *Multiple Bonds Between Metal Atoms*; Wiley: New York, 1982; and references therein.
(2) Cotton, F. A.; Walton, R. A. *Struct. Bonding* **1985**, *62*, 1–49.
(3) Mathisen, K. B.; Wahlgren, U.; Pettersson, L. G. M. *Chem. Phys. Lett.* **1984**, *104*, 336–342 and references therein.
(4) Hay, P. J. *J. Am. Chem. Soc.* **1982**, *104*, 7007–7017 and references therein.
(5) Goddard, W. A., III; Ladner, R. C. *J. Am. Chem. Soc.* **1971**, 93, 6750–6756.
(6) Bobrowicz, F. W.; Goddard, W. A., III In *Modern Theoretical Chemistry: Methods of Electronic Structure Theory*; Schaefer, H. F., III, Plenum: New York, 1977; Vol. 3, Chapter 4, pp 79–127.

0002-7863/87/1509-5580$01.50/0 